SERBIAN JOURNAL OF ELECTRICAL ENGINEERING
Vol. 16, No. 3, October 2019, 359-376

UDC: 620.92:621.383.51 **DOI: https://doi.org/10.2298/SJEE1903359G**

State Estimation of the Voltage Conversion Process in a Solar Power System with Kalman Filter

Milan Gojković[1], Đorđe Damnjanović[2], Radojka Krneta[2], Dejan Vujičić[2], Marina Milošević[2]

Abstract: The state estimation of the voltage conversion process (with Kalman filtering) in a solar power system is shown in this paper. Theoretical principles of solar power systems are presented, along with the position and working principles of a DC-DC boost converter in a solar power system. Different modes of state estimation of the voltage conversion process are shown, along with a detailed explanation of the Kalman filter appliance. This approach can be applied to one of the maximum power point tracking systems (MPPT). In the practical section of this paper, the implementation of noise filtering concepts in a solar power system is shown, by using the National Instruments LabVIEW programming suite. Processes that occur in this type of system are simulated, and the basic principles of noise cancellation are explained, in order to achieve optimal working conditions.

Keywords: Boost Converter, Kalman Filter, Maximum Power Point Tracking System, Solar Power System, State Estimation.

1 Introduction

Alternative or renewable energy sources, such as the energy of the Sun, wind or biomass, only represent a small percentage of the world's production of electrical energy at the moment. Usually, energy from fossil fuels, rivers, and nuclear sources are used. Greater usage of alternative energy sources would allow the world greater ecological progress, since these are "clean" methods of energy production.

In this paper, special attention is given to energy from the Sun and the possibility of its exploitation. The possibilities for the utilisation of solar energy are numerous, but this type of energy currently comprises less than of 1% of global consumption of electrical energy.

When speaking of radiation energy from the Sun, it is implied that its utilisation is immediate when it reaches the Earth, i.e. that there is immediate

[1]Digital Share, Miloja Pavlovića 9, 34000 Kragujevac, Serbia; E-mail: milan.gojkovic@digitalshare.eu
[2]University of Kragujevac, Faculty of Technical Sciences Čačak, Sv. Save 65, Čačak, Serbia;
E-mails: radojka.krneta@ftn.kg.ac.rs; dejan.vujicic@ftn.kg.ac.rs; djordje.damnjanovic@ftn.kg.ac.rs

utilisation of the Sun's radiation. The flow of the Sun's energy is called the solar constant, which is 1,400 W/m^2 at the Earth's average distance from the Sun, with an angle of incidence of 90^o, disregarding atmospheric absorption.

As it passes through the atmosphere, part of the energy is disbursed by complex processes and another part is reflected and re-emitted into space. The average energy flow due to atmospheric absorption and disruption is 230 W/m^2 (or 5.52 kWh/m^2, daily). These are, of course, average values and the actual values depend on the latitude, time of day, cloud appearance, pollution etc. [1].

A solar power system consists of a solar panel (which transforms the thermal energy of the Sun into electrical energy), a distributive system, and the consumers that use the energy produced. In order to optimise the process of electrical energy production in the solar power system, the negative effects of noise, which is inevitably created in these systems, have to be annulled or, at least, mitigated as much as possible. Noise degrades the characteristics of the output parameters and inter-parameters, which results in lower utilisation of the system. Filtration or de-noising is, therefore, a necessary process in a solar power system.

Some of the advantages of using solar cells can be outlined. Solar cells convert solar energy into electric energy directly, without moving mechanical parts, they are environmentally friendly, and they demand only minimal maintenance over a working period of some twenty years.

Unfortunately, there are also disadvantages with using solar cells. There is only an immediate production of electric energy, i.e. only in the period of the radiation and it is proportional to the magnitude of the Sun's radiation; the density of the force they produce is small (100 W/m^2 at best) but their price is high and their utilisation percentage is low (approximately 15%). The second disadvantage is low energetic profitability. Namely, the production of these cells demands a particularly high consumption of expensive materials (aluminium, silicon, and copper) so that the time of retrieval of the invested energy is around 20 years.

The usage of Kalman filter in the filtration of the signals obtained from the solar panel (as a part of the solar power system), is shown in this paper. The state estimation of the voltage conversion process in a solar power system was carried out by the simulation of the conditions that exist in a solar power system. Special attention was given to the processes occurring in the boost converter, which is modelled in state space. It will be shown that Kalman filter can be successfully used to estimate the state of the process of voltage conversion in the boost converter, as part of the solar power system. Also, the noise that is present in the system can be successfully filtered to diminish its effects. All of these topics were realised in a solar power system simulation, using LabVIEW. With this in mind, the simulator presented in this paper can be

used as an additional technique in one of the MPPT (Maximum Power Point Tracking) algorithms.

The remainder of the paper is organised as follows. The second section describes related work, in terms of MPPT systems. The third section provides a brief introduction to the operating principle of the photovoltaic cell. The fourth section presents the state space model of the voltage conversion process in the boost converter, as part of the solar power system. The working principle of the boost converter is described, as well as the state space model. System analysis and specifications are presented in the fifth section. The sixth section describes the simulator software. Together with the appearance of the application, the crucial software blocks were described: the state space model of the voltage conversion process, Kalman filter realisation, and the system output. The final section summarises the work presented in this paper and gives some directions for future work.

2 Related Work

The maximum power point tracking systems (MPPT) provide a way of achieving maximum power at the output by controlling various parameters and one of those parameter is the output voltage.

One of the components of the solar power system is the DC/DC converter. It is very important to have the best suited type of converter in a solar power system. In [2], three basic topologies of DC/DC converters with resistive loads connected to photovoltaic modules were analysed. These are the:

– Module-buck converter-load configuration,

– Module-boost converter-load configuration, and

– Module-buck/boost converter-load configuration.

It is shown that the buck-boost DC/DC converter topology is the only one that allows for following up the PV (Photovoltaic) module maximum power point (MPP) regardless of temperature, irradiance and connected load.

Some authors [3] have proposed ways of grouping methods that place the MPP from a PV generator into either direct or indirect methods. Indirect methods estimate MPP from measurements of the PV generator's voltage, current PV, and the irradiance, or by using empirical data in mathematical expressions. The second group are the direct methods that obtain the actual maximum power from the measurements of the PV generator's voltage and current PV.

In [4], a comparison of MPPT techniques was carried out. Authors give 19 different methods with various characteristics, such as dependency on PV array, analogue or digital measurements, periodic tuning, convergence speed, implementation complexity, and sensed parameters etc.

The method of terminal sliding mode control (TSMC) for maximum power tracking of PV power systems is described in papers [5] and [6]. In [5], a TSMC-based controller is developed to regulate the system to the searched reference MPP. In [6] the PV array output power is measured and, based on that, the duty cycle of the DC/DC converter control signal is changed.

In papers [7] and [8], the authors propose the use of an artificial neural network as an MPP tracking method. This method shows more stability and more accuracy compared to conventional methods.

A fuzzy logic controller is proposed in papers [9 – 15], as a solution to the MPP tracking problem. It uses a sampling measure of the PV array power and voltage and then determines the optimal increment required to achieve the best operating voltage, this then allows maximum power tracking. Initial tuning parameters of the fuzzy logic system are extracted from expert knowledge using a model of a PV module under varying solar radiation, temperature, and load conditions. Fuzzy logic can determine the size of the perturbed voltage and minimise voltage variations.

These solutions (as well as the solution described in this paper) can be used to improve the efficiency of Serbian energy systems, whose current condition is unsatisfactory [16].

3 Operating Principle of Photovoltaic Cell (Photovoltaic Effect)

The photovoltaic (PV) cell is the core block of the photovoltaic system. It represents the *p-n* junction, which converts the Sun's radiation into electric energy by using the photovoltaic effect. It comprises a semiconductor material, usually silicon. Due to the absorption of solar radiation, electron-cavity pairs are created in the *p-n* junction. Due to the Sun's radiation (inside or close to the *p-n* junction), the inner electric field separates the electrons and the cavities. Thereby, the electrons move towards the *n* side while the cavities go towards the *p* side of the *p-n* junction and, as a consequence of the movement, there is a potential difference, i.e. the voltage. When the PV cell is connected to the circuit, the current will flow through to the consumer [17 – 20]. Fig. 1 illustrates the operating principle of the photovoltaic cell.

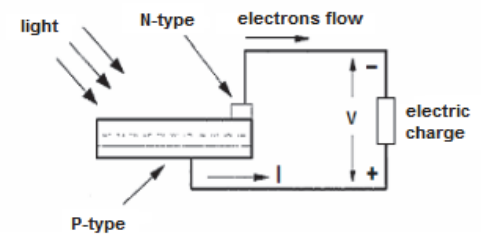

Fig. 1 – *Operating principle of the photovoltaic cell.*

The illuminated PV cell acts as the source of the perpetuate current. Its equivalent scheme is shown in Fig. 2. The source of the perpetuate current is linked to the diode in a parallel way. The serial impedance R_s represents the resistance of the *p-n* junction and it depends on the material that the PV cell is made of and needs to have as low a resistance as possible. The parallel impedance R_p comes from the micro-effects and impurities on the inside of the PV cell and depends on the characteristics of the cell; it is usually large enough to be considered infinite. The typical values for R_s and R_p, for silicon PV cells are: R_s<0.1Ω and R_p > 500Ω.

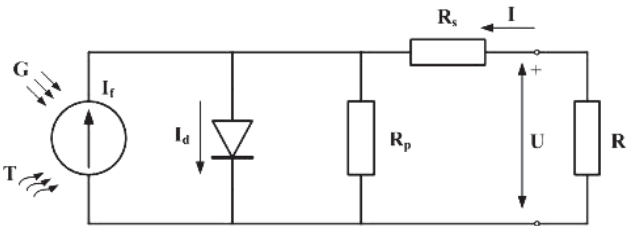

Fig. 2 – *The equivalent scheme of the photovoltaic cell.*

Based on the given equivalent scheme of the PV cell and with certain omissions ($R_s = 0$ and $R_s \to \infty$), we can give the equation for the outgoing current *I*:

$$I = I_f - I_d = I_f - I_0(e^{\frac{qU}{kT}} - 1), \tag{1}$$

where:

– I_0 – invert current of the diode saturation,

– I_f – generated photocurrent,

– *U*, *I* – outgoing voltage and current, respectively.

The most important part of the PV cell, is its working area when it produces electric energy. Because of this, only this area is usually drawn in a PV cell characteristic diagram, assuming the values of the current to be positive (Fig. 3). The surface of the striped rectangle $U_m I_m$, is equal to the maximum force the cell can produce.

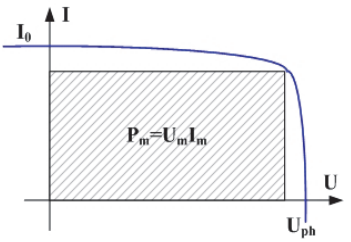

Fig. 3 – *Usual representation of the U-I characteristic of the PV cell.*

4 State Space Model of the Voltage Conversion Process in the Solar Power System Using the Boost Converter

A boost converter is a kind of DC-DC converter with a value of output voltage higher than the value of the input voltage. They are widely used with solar power systems (usually connected to the solar plate) in order to get higher amplitudes of output voltage. A boost converter is representative of a class of switching power units with two semiconductor switches (transistor and diode) that has at least one silencer or a capacitor. The diode serves as the alternative branch for the closing of the circuit when the transistor is off and the silencer stores the energy [21 – 28].

4.1 Working principle of the boost converter

The key principle of the boost converter is based on the tendency of the coil to resist the change of current. In the boost converter, the output voltage is always larger from the input voltage. The scheme of the boost converter is shown in Fig. 4. When the switch is on (ON), the electricity flows through the coil and it accumulates energy. When the switch is off (OFF), the coil tends to empty itself so that the polarity of the voltage on the coil changes and is added to the input voltage. This being done, the voltage on the coil and the input voltage are linked in series and, together, they cause the output capacitor on the voltage to be larger than the input voltage [26].

The main principle of the boost converter consists of two different states (Fig. 5).

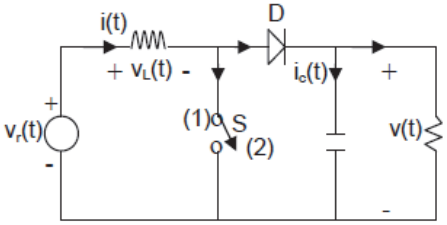

Fig. 4 – *The scheme of the boost converter.*

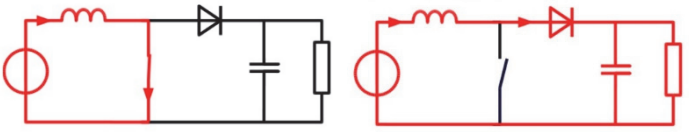

(a) (b)

Fig. 5 – *The main principle of the boost converter:*
(a) *the switch is on (ON);* (b) *the switch is off (OFF).*

In the ON state, the switch S (Fig. 4) is closed, which enlarges the current of the coil. In the OFF state, the switch is open and the only path that the current

in the coil can travel is over the invert diode D, capacitor C and the resistance R. The result is the transfer of the energy located in the capacitor during the ON state.

4.2 State space model of the boost converter

For a typical DC-DC boost converter (shown in Fig. 4), the output voltage is defined by the following equation:

$$v(t) = \frac{1}{1-d} v_r(t), \tag{2}$$

where d is duty cycle, and is calculated in the following way:

$$d = \frac{t_{on}}{t_{on} + t_{off}}. \tag{3}$$

The state space technique can be used to describe the behaviour of the DC-DC boost converter which produces the exit based on the behaviour of the signals in the switching converter, over the set of linear, time-invariant equations in the state space. Those equations were retrieved by continual functions of modulation of the relations between the signals [21 – 23]. The operations in the space state are described with the equation of the state and the exit equation, given in (4):

$$\dot{x}(t) = Ax(t) + Bu(t), \qquad y(t) = Cx(t) + Du(t). \tag{4}$$

In (4) $\dot{x}(t)$ is the first derivate of the state vector $x(t)$ and $u(t)$ is an input vector, and $y(t)$ is an output vector, while the variables A, B, C, and D are corresponding matrices.

The state variables are the input current $i(t)$ and the output voltage $v(t)$, so that the defined state vector can be described as:

$$x(t) = \begin{bmatrix} i(t) \\ v(t) \end{bmatrix}. \tag{5}$$

The independent source $v_r(t)$ is taken as the input vector and also the voltage drop on the V_d diode, so that the input vector $u(t)$ can be written thus:

$$u(t) = \begin{bmatrix} v_r(t) \\ V_d \end{bmatrix}. \tag{6}$$

It is necessary to determine the input current $i_r(t)$ for the converter model. In order to calculate this current, it is necessary to add it to the output vector $y(t)$, so the output vector can be written like this:

$$y(t) = \left[i_r(t) \right]. \tag{7}$$

When the switch S is in position 1 (Fig. 4), we get the scheme shown in Fig. 6.

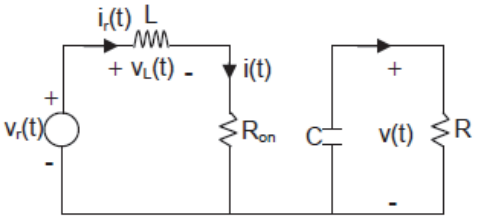

Fig. 6 – *The scheme of the boost converter during the first interval.*

In Fig. 6, the switch is modelled with some resistance R_{on} that has a very small value and can be ignored. Using Kirchhoff's laws, we get the following equations:

$$\begin{gathered} v_r(t) - L\frac{\mathrm{d}i(t)}{\mathrm{d}t} - R_{on}i(t), \\ \frac{\mathrm{d}i(t)}{\mathrm{d}t} = \frac{1}{L}v_r(t) - \frac{R_{on}}{L}i(t), \\ C\frac{\mathrm{d}v(t)}{\mathrm{d}t} = -\frac{v(t)}{R} \quad \Rightarrow \quad \frac{\mathrm{d}v(t)}{\mathrm{d}t} = -\frac{v(t)}{RC}, \\ i_r(t) = i(t), \end{gathered} \tag{8}$$

where the state space model is:

$$\begin{gathered} \frac{\mathrm{d}}{\mathrm{d}t}\begin{bmatrix} i(t) \\ v(t) \end{bmatrix} = \begin{bmatrix} -\dfrac{R_{on}}{L} & 0 \\ 0 & -\dfrac{1}{RC} \end{bmatrix}\begin{bmatrix} i(t) \\ v(t) \end{bmatrix} + \begin{bmatrix} \dfrac{1}{L} & 0 \\ 0 & 0 \end{bmatrix}\begin{bmatrix} v_r(t) \\ V_d(t) \end{bmatrix}, \\ \begin{bmatrix} i_r(t) \end{bmatrix} = \begin{bmatrix} 1 & 0 \end{bmatrix}\begin{bmatrix} i(t) \\ v(t) \end{bmatrix} + \begin{bmatrix} 0 & 0 \end{bmatrix}\begin{bmatrix} v_r(t) \\ V_d(t) \end{bmatrix}. \end{gathered} \tag{9}$$

When the switch S moves from position 1 into position 2 (Fig. 4), we get the scheme of the boost converter as shown in Fig. 7.

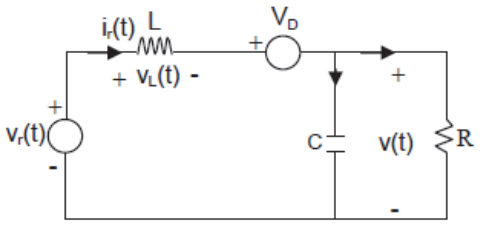

Fig. 7 – *The scheme of the boost converter during the second interval.*

Using Kirchhoff's laws, we get the following equations:

$$v_r(t) - L\frac{\mathrm{d}i(t)}{\mathrm{d}t} - V_d - v(t) \quad \Rightarrow \quad \frac{\mathrm{d}i(t)}{\mathrm{d}t} = \frac{1}{L}v_r(t) - \frac{1}{L}V_d - \frac{1}{L}v(t),$$
$$C\frac{\mathrm{d}v(t)}{\mathrm{d}t} = i(t) - \frac{v(t)}{R} \quad \Rightarrow \quad \frac{\mathrm{d}v(t)}{\mathrm{d}t} = \frac{1}{C} - \frac{v(t)}{RC}, \tag{10}$$
$$i_r(t) = i(t).$$

From (10) follows:

$$\frac{\mathrm{d}}{\mathrm{d}t}\begin{bmatrix} i(t) \\ v(t) \end{bmatrix} = \begin{bmatrix} 0 & -\frac{1}{L} \\ -\frac{1}{C} & -\frac{1}{RC} \end{bmatrix}\begin{bmatrix} i(t) \\ v(t) \end{bmatrix} + \begin{bmatrix} \frac{1}{L} & -\frac{1}{L} \\ 0 & 0 \end{bmatrix}\begin{bmatrix} v_r(t) \\ V_d(t) \end{bmatrix},$$
$$[i_r(t)] = [1 \quad 0]\begin{bmatrix} i(t) \\ v(t) \end{bmatrix} + [0 \quad 0]\begin{bmatrix} v_r(t) \\ V_d(t) \end{bmatrix}. \tag{11}$$

The values of the matrices A, B, C, and D are calculated as follows:

$$\begin{aligned} A &= DA_1 + DA_2, \\ B &= DB_1 + D'B_2, \\ C &= DC_1 + D'C_2, \\ D &= DD_1 + D'D_2, \end{aligned} \tag{12}$$

where:

$$D = 1 - D'. \tag{13}$$

So, from (12) and (13) we get:

$$A = D\begin{bmatrix} -\frac{R_{on}}{L} & 0 \\ 0 & -\frac{1}{RC} \end{bmatrix} + D'\begin{bmatrix} 0 & -\frac{1}{L} \\ -\frac{1}{C} & -\frac{1}{RC} \end{bmatrix} = \begin{bmatrix} -\frac{R_{on}D}{L} & -\frac{D'}{L} \\ -\frac{D'}{C} & -\frac{1}{RC} \end{bmatrix}, \tag{14}$$

$$B = D\begin{bmatrix} \frac{1}{L} & 0 \\ 0 & 0 \end{bmatrix} + D'\begin{bmatrix} \frac{1}{L} & -\frac{1}{L} \\ 0 & 0 \end{bmatrix} = \begin{bmatrix} \frac{1}{L} & -\frac{D'}{L} \\ 0 & 0 \end{bmatrix}, \tag{15}$$

$$C = D\begin{bmatrix} 1 & 0 \end{bmatrix} + D'\begin{bmatrix} 1 & 0 \end{bmatrix} = \begin{bmatrix} 1 & 0 \end{bmatrix}, \tag{16}$$

$$D = D\begin{bmatrix} 0 & 0 \end{bmatrix} + D'\begin{bmatrix} 0 & 0 \end{bmatrix} = \begin{bmatrix} 0 & 0 \end{bmatrix}. \tag{17}$$

4.3 System analysis and specifications

For the purpose of estimating the states of the voltage conversion process in a solar power system and de-noising of its parameters, a software application was created. The state variables that were being analysed are input current (from the PV cell) and DC-DC converter output voltage. First of all, it is necessary to model the DC-DC converter process in order to choose a valid state estimator. Due to its fine characteristics for state estimation, Kalman filter was chosen. Its role is to perform consistent estimation of state variables, i.e. to eliminate noise in the system (both process noise and measurement noise).

The voltage from a solar cell/panel is applied to a DC-DC converter, which generates DC voltage. This DC voltage is used by the consumer to charge a battery, while the measurement system performs measurements of the system parameters. Precise and consistent voltage estimation of the DC-DC converter output is crucial.

The schematic presentation of the whole system is shown in Fig. 8.

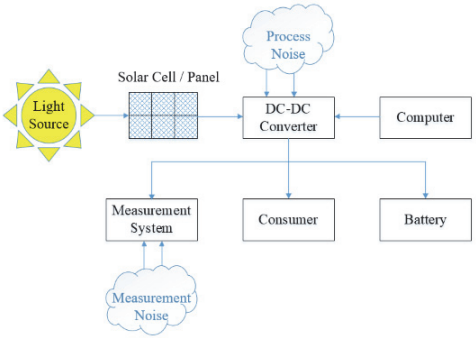

Fig. 8 – *The schematic presentation of the system.*

The application was realised by using Matlab/Simulink and LabVIEW software packages. These two software tools have a sufficient number of embedded block functions for state estimation. By using those block functions, the user can create a relatively simple application that is capable of doing state estimation and de-noising of the parameters in the solar power system.

4.4 Software realisation of the voltage conversion process state estimator in the solar power system

The estimation of the state variables during the process of conversion in the solar power system is carried out by using the LabVIEW application, wherein two state variables are being observed: the current on the input of the converter and the voltage on the output. The conversion process is described with the

model in the state space. Based on this known DC voltage, Kalman filter (whose role is to remove noise from the process and measurement noise from the system) is applied on the entrance that is polluted with Gaussian white noise. The system is expected to have some load attached. It will be turned on when the output voltage reaches 12V and shut off will happen when the output voltage reaches 15V. The simulation was carried out based on commercially available development systems, that have the capability to charge batteries and which usually demand an input voltage from between 12V to 15V.

Some of the LabVIEW modules, such as Programming, Mathematics, Signal Processing, Data Communication, Control Design & Simulation, were used for designing the application. The user interface of the application used in LabVIEW is shown in Fig. 9.

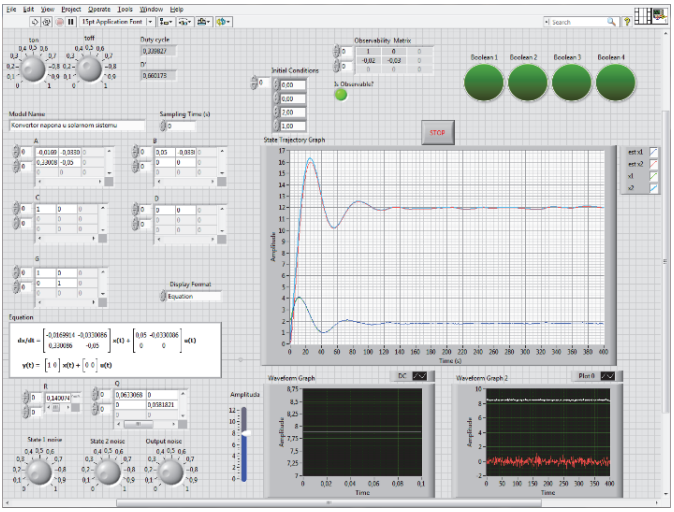

Fig. 9 – *User interface of the application made in LabVIEW.*

4.5 The state space model of the voltage conversion process

The state space model is realised by using the block function "CD Construct State-Space Model.vi" within the Control Design & Simulation Design module (Fig. 10).

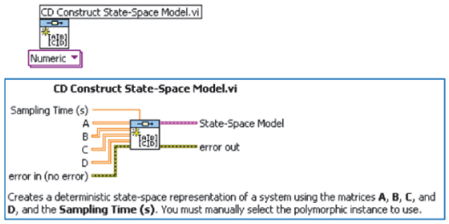

Fig. 10 – *Block function for state space model.*

The realisation of the state space model is shown in Fig. 11.

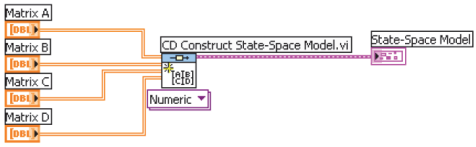

Fig. 11 – *The realisation of the state space model.*

The values of the matrices A, B, C, and D can be entered manually in the Front panel, but within the realised application, the entry of the matrices is solved by the program. The first part is defining time t_{on} and t_{off} that show how much time the switch was on and off inside the converter. According to (3), the duty cycle D is calculated. Based on the values of the parameters L_{min} and C_{min}, the optimal value of the duty cycle is 0.33 [29]. Judging by the physical characteristics of the boost converter, the upper limit of the output voltage at which the boost converter works normally is 24V [30]. According to (14) and the values of L = 20mH, C = 2mF and R = 10Ω, we get the values of the matrices and the state space model equations.

Time values t_{on} and t_{off} can be changed within a single time interval, so we can keep track of what happens to the values of the matrices.

4.6 Observability

The necessary condition for Kalman filter to work properly is that the system, whose conditions need to be estimated, needs to be observable. So, the observability should be checked before using Kalman filter.

The matrix of observability is defined as:

$$Q_o = \begin{bmatrix} C \\ CA \\ \vdots \\ CA^{n-1} \end{bmatrix}, \tag{18}$$

where n is the order of the system (the number of the conditions of state space model).

The needed and sufficient condition for a system to be observable is that the range of the matrix of observability Q_o is equal to the order of the system n.

4.7 Estimation

Kalman filter assumes that there is a time discrete process, which is observed or managed. The Kalman filter works by calculation of the estimated states $\hat{x}(t)$, based on the noisy measurements y_k, for the random process x_k, described with linear discrete model in the state space. Kalman's filter, as the

optimal estimator and the predictor of the unknown value, has been extensively used in system management, navigation, tracking and prediction of the object trajectory [31 – 33].

After the given state space model, the conversion process and the observability check, it is possible to apply Kalman filter. First, we need to get Kalman gain, which leads to the function of the state estimation. The function used for obtaining the Kalman gain is "CD Kalman Gain.vi". Fig. 12 shows the function block location in the realised system.

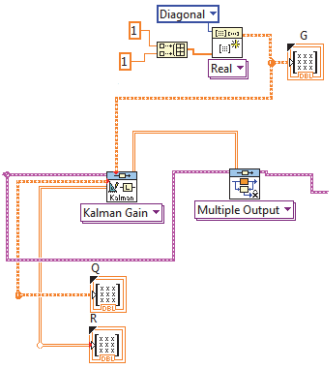

Fig. 12 – *Place of the function block for the Kalman's amplification.*

From Fig. 12, it can be seen that it is necessary to define the matrices *G*, *Q* and *R*. Wherein:

– Matrix *G* is the matrix of the amplification of the process noise and is represented with the identity matrix I.

– Matrix of the process noise (*Q*) and the matrix of the measurement noise (*R*) are represented as follows:

$$G=\begin{bmatrix}1&0&0&0\\0&1&0&0\\0&0&\ddots&0\\0&0&0&1\end{bmatrix},\quad Q=\begin{bmatrix}q_{11}&0&0&0\\0&q_{22}&0&0\\0&0&\ddots&0\\0&0&0&q_{nn}\end{bmatrix},\quad R=\begin{bmatrix}r_{11}&0&0&0\\0&r_{22}&0&0\\0&0&\ddots&0\\0&0&0&r_{nn}\end{bmatrix}. \tag{19}$$

wherein q_{ij} and r_{ij} are the co-variances of the process and measurement noises.

Within the realised application, the function "CD State Estimator.vi" was used, which can be found in the Control Design & Simulation module. Fig. 13 shows the location of the block function for the estimation of the process state.

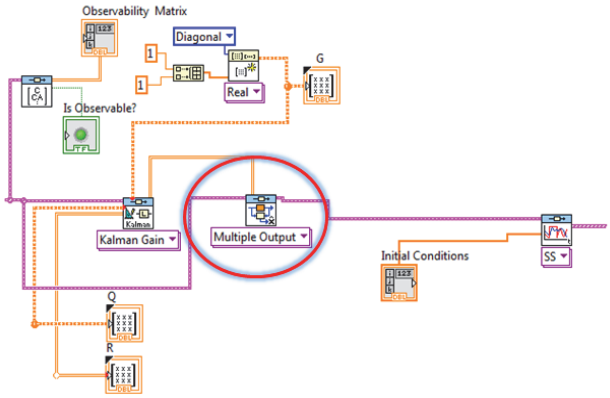

Fig. 13 – *Location of the block function for the estimation of the process state.*

4.8 System output

A DC voltage from the solar panel, which is simulated with an amplitude that can vary from 0V to 12V within this application, is brought to the input of the converter in the solar power system (usually the voltage is from 8V to 12V). The voltage is noised on the process input, and the measurement noise is added to it at the exit; the role of the application is, based on the noised sources, to estimate the input current and the output voltage of the converter. Fig. 14 shows the system output based on the noised input signals.

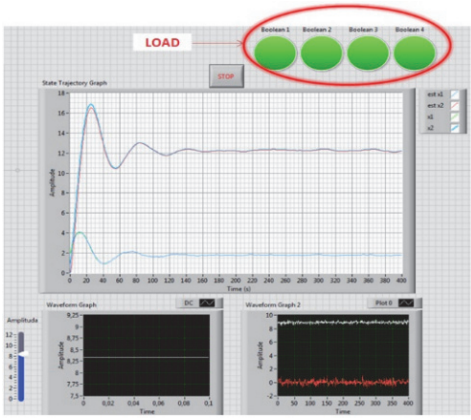

Fig. 14 – *Display of the system output.*

On the Waveform Graph, the input voltage with an amplitude of approximately 8.3V is shown (the amplitude can be changed into time values by using the amplitude controls). The Waveform Graph shows the noisy input voltage (marked in white) and the noisy input current (marked in red).

On the State Trajectory Graph, four signals are shown. The red colour marks the estimation of the voltage state on the output, while the light blue colour signifies the output voltage. The dark blue line shows the estimation of the current state on the input and the green line, the current on the entrance (Fig. 15).

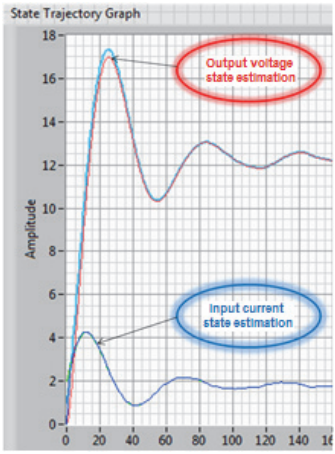

Fig. 15 – *Estimation of the state variables.*

Fig. 14 also shows the load (simulated with four diodes) which are momentarily switched on, because the output voltage reached 12V, and will be switched off when the output voltage reaches 15V.

As can be seen from Fig. 14, Kalman filter has made a consistent estimation of the state variables in the system based on the noisy sources, which was the main goal of the filtering in the first place.

5 Conclusion and Future Work

In this paper, we presented the software-realised simulator of the solar power system. Special attention has been paid to the use of Kalman filter as the estimator of the state of the system. An estimator is used on the processes that happen in the boost converter, as one of the components of the solar panel. The role of the boost converter in a solar power system is to regulate the voltage levels.

The simulator was made in the LabVIEW software suite. Its ease of use and multitude of functions facilitated the realisation of the simulator. The boost

converter was modelled in state space and white Gaussian noise was introduced to the system. At the same time, Kalman filtering was successful in the estimation of the state space voltage conversion process in the boost converter and in the diminution of the noise.

The main advantage of this simulation model is the easiness of the system state readings and their visual display. A final user would not need much time to adjust to how the system works and to easily change the parameters and the results.

Future work on this system can be described as usage of real-time signals and monitoring their behaviour. The work presented in this paper represents a theoretical and simulation model of the state space estimation of processes in a solar power system. Having the appropriate hardware equipment means that the realised algorithm of estimation can be tested in practice.

The realised model is meant to assist in the estimation of the states in the boost converter of the solar panel, as one of the components of the solar power system. By upgrading the model, it is possible to affect the states in the other parts of the solar panel and even the whole solar power system. It could be possible to affect the states of the inverter system in the solar panel, as well as the noise filtration in the distributive part of the system. Also, the states of the attached load could also be monitored in order to further optimise the whole process. Based on the idea of future development, this approach can be suitable for usage in one of the algorithms of maximum power tracking.

6 References

[1] D. Chiras, R. Aram, K. Nelson: Power from the Sun, Practical Guide to Solar Energy, New Society Publishers, Vankuver, Canada, 2009.

[1] J. M. Enrique, E. Durán, M. Sidrach-de-Cardona, J. M. Andújar: Theoretical Assessment of the Maximum Power Point Tracking Efficiency of Photovoltaic Facilities with Different Converter Topologies, Solar Energy, Vol. 81, No. 1, January 2007, pp. 31 – 38.

[2] V. Salas, E. Olías, A. Barrado, A. Lázaro: Review of the Maximum Power Point Tracking Algorithms for Stand-Alone Photovoltaic Systems, Solar Energy Materials and Solar Cells, Vol. 90, No. 11, July 2006, pp. 1555 – 1578.

[3] T. Esram, P. L. Chapman: Comparison of Photovoltaic Array Maximum Power Point Tracking Techniques, IEEE Transactions on Energy Conversion, Vol. 22, No. 2, June 2007, pp. 439 – 449.

[4] C.- S. Chiu, Y.- L. Ouyang, C.- Y. Ku: Terminal Sliding Mode Control for Maximum Power Point Tracking of Photovoltaic Power Generation Systems, Solar Energy, Vol. 86, No. 10, October 2012, pp. 2986 – 2995.

[5] D. Rekioua, A. Y. Achour, T. Rekioua: Tracking Power Photovoltaic System with Sliding Mode Control Strategy, Energy Procedia, Vol. 36, 2013, pp. 219 – 230.

[6] R. Noroozian, F. Barzideh, A. Jalilvand: A Novel Maximum Power Point Tracking Method for PV Systems Using Artificial Neural Network, Engineering Intelligent Systems, Vol. 21, No. 4, December 2013, pp. 239 – 247.

[7] V. Lo Brano, G. Ciulla, M. Di Falco: Artificial Neural Networks to Predict the Power Output of a PV Panel, International Journal of Photoenergy, Vol. 2014, Article ID 193083, pp. 1 – 12.

[8] S. Lalouni, D. Rekioua, T. Rekioua, E. Matagne: Fuzzy Logic Control of Stand-Alone Photovoltaic System with Battery Storage, Journal of Power Sources, Vol. 193, No. 2, September 2009, pp. 899 – 907.

[9] I. H. Altas, A. M. Sharaf: A Novel Maximum Power Fuzzy Logic Controller for Photovoltaic Solar Energy Systems, Renewable Energy, Vol. 33, No. 3, March 2008, pp. 388 – 399.

[10] M. Taherbaneh, A. H. Rezaie, H. Ghafoorifard, K. Rahimi, M. B. Menhaj: Maximizing Output Power of a Solar Panel via Combination of Sun Tracking and Maximum Power Point Tracking by Fuzzy Controllers, International Journal of Photoenergy, Vol. 2010, Article ID 312580, pp. 1 – 13.

[11] S. Subiyanto, A. Mohamed, H. Shareef: Hopfield Neural Network Optimized Fuzzy Logic Controller for Maximum Power Point Tracking in a Photovoltaic System, International Journal of Photoenergy, Vol. 2012, Article ID 798361, pp. 1 – 13.

[12] C. S. Chin, P. Neelakantan, H. P. Yoong, K. T. K. Teo: Control and Optimization of Fuzzy Based Maximum Power Point Tracking in Solar Photovoltaic System, Proceedings of the 4th Global Conference on Power Control and Optimization, Kuching, Malaysia, December 2010, pp. 1 – 6.

[13] C.- L. Liu, J.- H. Chen, Y.- H. Liu, Z.- Z. Yang: An Asymmetrical Fuzzy-Logic-Control-Based MPPT Algorithm for Photovoltaic Systems, Energies, Vol. 7, No. 4, April 2014, pp. 2177 – 2193.

[14] C. P. Roy, D. Vijaybhaskar, T. Maity: Modelling of Fuzzy Logic Controller for Variable-Step MPPT in Photovoltaic System, Proceedings of the IEEE 1st International Conference on Condition Assessment Techniques in Electrical Systems (CATCON), Kolkata, India, December 2013, pp. 341 – 346.

[15] D. Gvozdenac, M. Kljajić, B. Gvozdenac-Urošević: Serbian Energy Efficiency Problems, Thermal Science, Vol. 18, No. 3, 2014, pp. 683 – 694.

[16] C. S. Solanki: Solar Photovoltaics: Fundamentals, Technologies and Applications, 2nd edition. Prentice-Hall of India Pvt. Ltd., New Delhi, India, 2011.

[17] J. A. Duffie, W. A. Beckman: Solar Engineering of Thermal Processes, 4th edition, John Wiley & Sons, Inc., Hoboken, New Jersey, USA, 2013.

[18] P. Kulišić, J. Vuletin, I. Zulim: Solar Cells, Školska knjiga, Zagreb, Croatia, 1994. (In Croatian).

[19] T. Surek: Solar Electricity, Progress and Challenges, National Renewable Energy Laboratory Golden, 2006.

[20] B. Johansson: Improved Models for DC-DC Converters, Media-Tryck Lund University, Lund, Sweden, 2003.

[21] C. A. Nwosu, M. Eng: State-Space Averaged Modeling of a Nonideal Boost Converter, The Pacific Journal of Science and Technology, Vol. 9, No. 2, November 2008, pp. 302 – 308.

[22] J. Zhang: Bidirectional DC-DC Power Converter Design Optimization, Modeling and Control, PhD Dissertation, Virginia Polytechnic Institute and State University, Blacksburg, USA, 2008.

[23] M. S. Jamri, T. C. Wei: Modeling and Control of a Photovoltaic Energy System Using the State-Space Averaging Technique, American Journal of Applied Sciences, Vol. 7, No. 5, May 2010, pp. 682 – 691.

[24] Q. Liu: Modular Approach for Characterizing and Modeling Conducted EMI Emissions in Power Converters, PhD Dissertation, Virginia Polytechnic Institute and State University, Blacksburg, USA, 2005.

[25] S. Kasat: Analysis, Design and Modeling of DC-DC Converter Using Simulink, Master Thesis, Graduate College of the Oklahoma State University, Oklahoma, USA, 2004.

[26] B. V. Sreenivasappa, Y. Udaykumar: Elimination of Output Voltage Oscillations in DC-DC Converter Using PWM with PI Controller, Serbian Journal of Electrical Engineering, Vol. 7, No. 1, May 2010, pp. 57 – 68.

[27] G. Amer, S. S. Rao: Estimation of Reliability of a Interleaving PFC Boost Converter, Serbian Journal of Electrical Engineering, Vol. 7, No. 2, November 2010, pp. 205 – 216.

[28] P. Petrović: Power Electronics, Faculty of Technical Sciences Čačak, Čačak, Serbia, 2011. (in Serbian).

[29] S. Masri, P.- W. Chan: Development of a Microcontroller-Based Boost Converter for Photovoltaic System, European Journal of Scientific Research, Vol. 41, No. 1, February 2010, pp. 38 – 47.

[30] H. Mahmood, K. Natarajan: Parasitics and Voltage Collapse of the DC-DC Boost Converter, Proceedings of the Canadian Conference on Electrical and Computer Engineering, Niagara Falls, Canada, May 2008, pp. 273 – 278.

[31] G. Welch, G. Bishop: An Introduction to the Kalman Filter, University of North Carolina at Chapel Hill, TR 95-041, 2006.

[32] R. E. Kalman: A New Approach to Linear Filtering and Prediction Problems, Journal of Basic Engineering, Vol. 82, No. 1, March 1960, pp. 35 – 45.